JACS
JOURNAL OF THE AMERICAN CHEMICAL SOCIETY
pubs.acs.org/JACS
Article

Development of High-Specificity Fluorescent Probes to Enable Cannabinoid Type 2 Receptor Studies in Living Cells

Roman C. Sarott, Matthias V. Westphal, Patrick Pfaff, Claudia Korn, David A. Sykes, Thais Gazzi, Benjamin Brennecke, Kenneth Atz, Marie Weise, Yelena Mostinski, Pattarin Hompluem, Eline Koers, Tamara Miljuš, Nicolas J. Roth, Hermon Asmelash, Man C. Vong, Jacopo Piovesan, Wolfgang Guba, Arne C. Rufer, Eric A. Kusznir, Sylwia Huber, Catarina Raposo, Elisabeth A. Zirwes, Anja Osterwald, Anto Pavlovic, Svenja Moes, Jennifer Beck, Irene Benito-Cuesta, Teresa Grande, Samuel Ruiz de Martín Esteban, Alexei Yeliseev, Faye Drawnel, Gabriella Widmer, Daniela Holzer, Tom van der Wel, Harpreet Mandhair, Cheng-Yin Yuan, William R. Drobyski, Yurii Saroz, Natasha Grimsey, Michael Honer, Jürgen Fingerle, Klaus Gawrisch, Julian Romero, Cecilia J. Hillard, Zoltan V. Varga, Mario van der Stelt, Pal Pacher, Jürg Gertsch, Peter J. McCormick, Christoph Ullmer, Sergio Oddi, Mauro Maccarrone, Dmitry B. Veprintsev, Marc Nazaré, Uwe Grether,* and Erick M. Carreira*

Cite This: *J. Am. Chem. Soc.* 2020, 142, 16953−16964

ABSTRACT: Pharmacological modulation of cannabinoid type 2 receptor (CB_2R) holds promise for the treatment of numerous conditions, including inflammatory diseases, autoimmune disorders, pain, and cancer. Despite the significance of this receptor, researchers lack reliable tools to address questions concerning the expression and complex mechanism of CB_2R signaling, especially in cell-type and tissue-dependent contexts. Herein, we report for the first time a versatile ligand platform for the modular design of a collection of highly specific CB_2R fluorescent probes, used successfully across applications, species, and cell types. These include flow cytometry of endogenously expressing cells, real-time confocal microscopy of mouse splenocytes and human macrophages, as well as FRET-based kinetic and equilibrium binding assays. High CB_2R specificity was demonstrated by competition experiments in living cells expressing CB_2R at native levels. The probes were effectively applied to FACS analysis of microglial cells derived from a mouse model relevant to Alzheimer's disease.

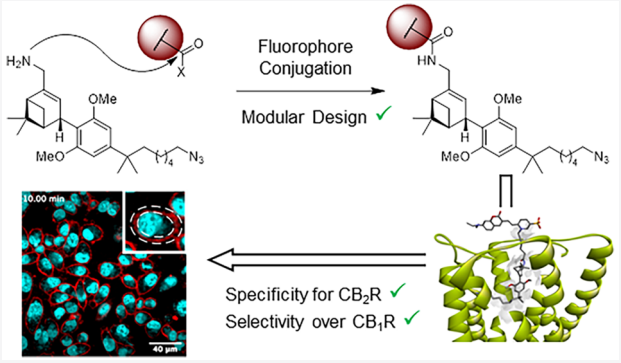

INTRODUCTION

There is currently great interest in the endocannabinoid system (eCB system) and associated signaling pathways in relation to the chemistry of life as well as in the context of developing new therapies. The eCB system is a complex lipid signaling network found in all vertebrates and consists of cannabinoid receptors (CBRs), their endogenous ligands (endocannabinoids), enzymes involved in ligand biosynthesis and degradation, as well as endocannabinoid transporters.[1] Cannabinoid type 1 and 2 receptors (CB_1R and CB_2R) are class A G-protein-coupled receptors (GPCRs) and have been shown to be involved in numerous physiological processes and disease states.[2−4] They share 44% overall and 68% homology in the ligand-binding domain.[3] Notably, CB_1R is the most abundant GPCR in the central nervous system (CNS) and mediates the psychotropic effects associated with *Cannabis* consumption mainly through the action of (−)-Δ^9-*trans*-tetrahydrocannabinol ((−)-Δ^9-THC).[5] CB_2R is predominantly expressed in the periphery, largely by cells of the immune system,[6,7] and is considered a highly promising target for the treatment of tissue injury and inflammation,[8,9] as well as neurodegenerative diseases such as Alzheimer's disease (AD) and multiple sclerosis.[10,11] Although several structurally distinct CB_2R agonists have shown promising

Received: May 22, 2020
Published: September 9, 2020

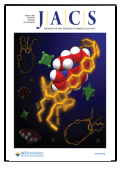

https://dx.doi.org/10.1021/jacs.0c05587
J. Am. Chem. Soc. 2020, 142, 16953−16964

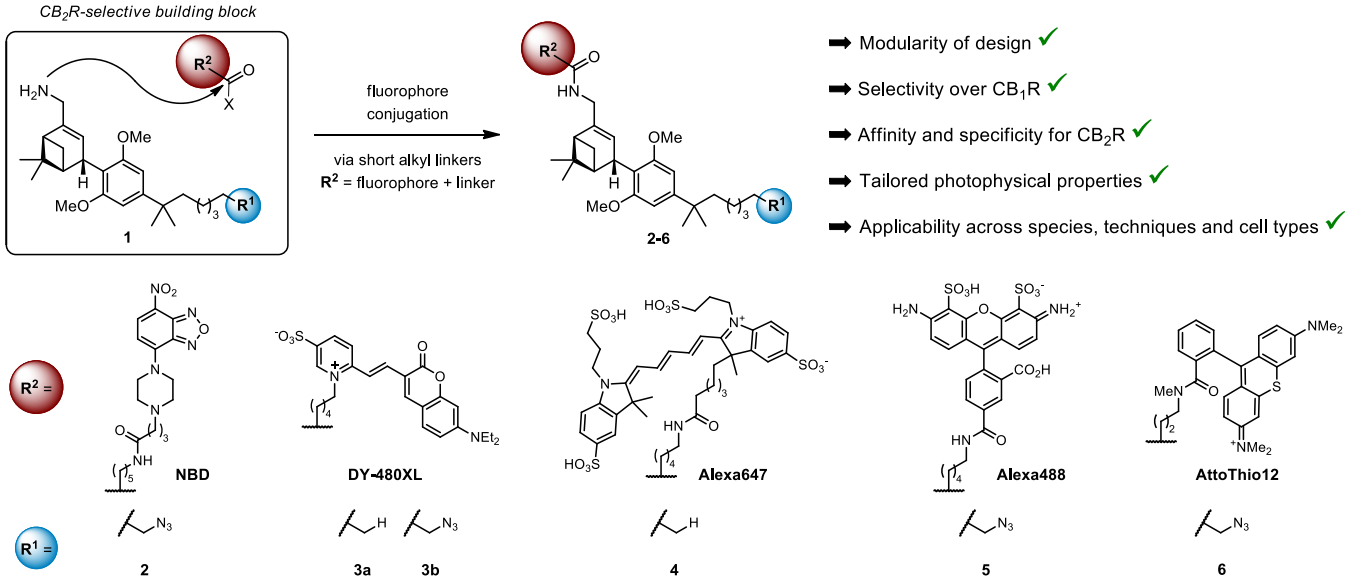

Figure 1. Modular design of CB_2R fluorescent probes. Attachment of fluorescent dyes to amine building block **1** via short linkers gives rise to CB_2R-selective fluorescent probes with bespoke photophysical properties.

Table 1. *In Vitro* Pharmacological Assessment of CB_2R Fluorescent Probes[a]

		K_i [nM]				EC_{50} [nM]			
compd	dye	hCB_2R	hCB_1R	mCB_2R	hK_i ratio (CB_1R/CB_2R)	hCB_2R	hCB_1R	mCB_2R	EC_{50} ratio (CB_1R/CB_2R)
2	NBD	4.2	>10 000	n.d.[b]	>2381	n.d.	n.d.	n.d.	n.d.
3a	DY-480XL	99	4031	1986	41	>10 000	>10 000	>10 000	n.d.
3b	DY-480XL	21	2378	1459	113	171 (150)	>10 000	118 (115)	>58
4	Alexa647	2565	>10 000	>10 000	>3.9	25 (109)	2152 (138)	370 (123)	86
5	Alexa488	268	>10 000	1 204	>37	n.d.	n.d.	n.d.	n.d.
6	AttoThio12	4.7	1075	1.1	228	5.6 (74)	>10 000	17 (73)	>1785

[a]Binding affinity (K_i) values were determined by a radioligand binding assay utilizing radioligand [^{3}H]-CP55,940 and membrane preparations from CHO cells overexpressing hCB_1R, hCB_2R, or mCB_2R. Forskolin-stimulated cAMP (EC_{50}) levels were measured using cells stably expressing hCB_2R, mCB_2R, or hCB_1R. Figures in parentheses correspond to efficacy expressed in % relative to 1 μM CP55,940. [b]n.d. = not determined.

effects in animal disease models, none has so far succeeded in the clinic,[12] stressing the need for better fundamental understanding of CB_2R chemistry, biology, and medicine.[10] The ability to address important questions is hampered by the lack of reliable biological tools such as receptor-specific antibodies,[13−15] and the highly inducible nature of CB_2R expression as a function of disease state[16−18] further complicates its biochemical and biophysical analysis.

Small-molecule-based probes will help to interrogate CB_2R function, mechanism of action, biased signaling, expression levels, and protein distribution in health and disease.[19] Of particular interest are fluorescent probes, which allow for real-time monitoring of ligand−receptor interactions and protein visualization with high spatiotemporal precision.[20−22] Several fluorescent ligands targeting CB_2R have been reported.[23−35] However, in our collective experience, the published probes perform less than optimally as judged by at least one of the following criteria: modularity of design for multiple applications, selectivity over CB_1R, affinity and specificity for CB_2R, photophysical properties, and applicability across species, techniques, and cell types. Furthermore, bifunctional probes that require additional manipulations prior to imaging are often incompatible with live cells.[36,37]

Recently, we reported the synthesis of HU-308-derived[38] primary amine **1** (Figure 1), which was linked via R^2 to residues such as alkynes, diazirines, azobenzene photoswitches, and 7-nitrobenzofurazan (NBD) dye (**2**). These were evaluated in limited *in vitro* pharmacology (CB_2R and CB_1R K_i, cAMP). However, the preliminary studies were largely synthetic in nature and did not assess **2** as a fluorescent probe. Herein, we report the modular synthesis and in-depth pharmacological evaluation of a series of CB_2R specific, high-affinity fluorescent probes. We also document their *in situ* application and validation in flow cytometry and real-time confocal microscopy of both living human and murine cells. Additionally, these probes proved effective in time-resolved fluorescence resonance energy transfer (TR-FRET)-based assays, allowing for determination of both binding affinities and kinetic parameters of CB_2R ligands without radiolabeled material. Finally, the probes are successfully applied to fluorescence-activated cell sorting (FACS) analysis of cells from a mouse model of Alzheimer's disease.

RESULTS AND DISCUSSION

Modular Probe Design and *in vitro* Pharmacology. With a high-affinity recognition element, such as **1**,[39] as a starting point, choices of the exit vector and linker-type for fluorophore attachment are the main challenges to ensure high probe affinity and selectivity.[40,41] Our preliminary synthetic studies with **2** suggested a strategy for a family of

https://dx.doi.org/10.1021/jacs.0c05587
J. Am. Chem. Soc. 2020, 142, 16953−16964

fluorescent probes.[42] Consequently, herein we report a series of probes **3a**–**6** in which the fluorescent dye was varied (Figure 1; for synthetic details, see the Supporting Information (SI)). Fluorophores DY-480XL,[43] Alexa647,[44] Alexa488,[45] and AttoThio12[46] were chosen for their large Stokes shift, red-shifted absorption and emission maxima with high extinction coefficient, suitability for FRET, and potential for ultra-high-resolution microscopy, respectively (for fluorescence spectra, see SI Figure S1 and Table S1). We focused on high-affinity azides **3b**, **5**, and **6**, as well as, for comparison, hydrocarbon analogs **3a** and **4**.

All fluorescent probes were subjected to *in vitro* pharmacological profiling in order to evaluate their affinity for CB_2R and selectivity over CB_1R (Table 1). Radioligand competition binding studies were performed with tritiated CP55,940 and membrane preparations of Chinese hamster ovary (CHO) cells overexpressing human (hCB_2R) or mouse CB_2R (mCB_2R), or human CB_1R (hCB_1R). Compounds **3a**, **3b**, **5**, and **6** showed high to excellent affinity to hCB_2R, exhibiting K_i values of 99, 21, 268, and 4.7 nM, respectively, as well as good selectivity over hCB_1R, with hCB_1R/hCB_2R K_i ratios of 41, 113, >37, and 228, respectively.[47] The presence of the terminal azide in **3b** led to significantly higher binding affinity for hCB_2R as well as boosted selectivity over hCB_1R when compared to **3a**. To the best of our knowledge, the high selectivity of **3b** and **6** for hCB_2R over hCB_1R is unprecedented for fluorescent CB_2R *agonists*, as discussed below.

In 2019 and 2020, X-ray and cryo-electron microscopy (cryo-EM) structures of antagonist- and agonist-bound CB_2R were reported.[48−50] We used the X-ray crystal structure of CB_2R in its active state, determined in complex with agonist WIN55,212,[49] in docking experiments of DY-480XL probe **3b**. The docking pose suggests that the fluorophore is positioned in the extracellular space (Figure 2). In addition,

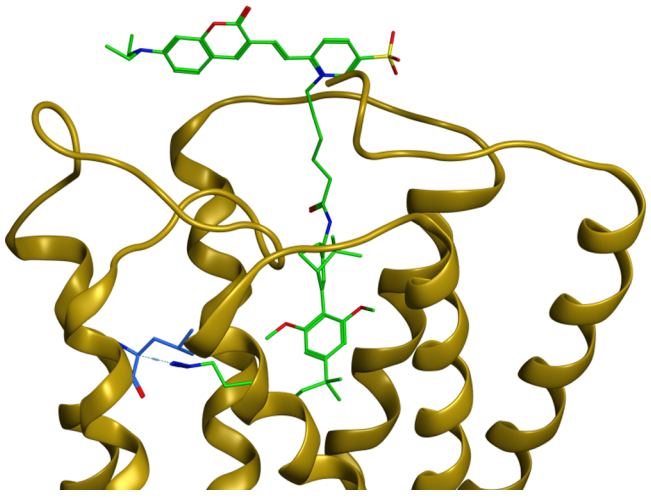

Figure 2. CB_2R docking studies. Probe **3b** was docked into active-state CB_2R crystal structure (PDB: 6PTO).

the azide of agonist **3b** is involved in a favorable H-bond with the $C_\alpha H$ of Leu191. This may explain the higher affinity of **3b** as well as of **6** as compared to probe **3a** carrying a hydrogen atom instead of an azide at the terminus of the alkyl side chain.

In functional studies, probe **3b** showed agonist activity with high efficacy (hCB_2R cAMP EC_{50} = 171 nM, %eff = 150). A comparable value for **3b**, EC_{50} = 133 nM, was obtained in a $[^{35}S]$GTP-γ-S G-protein activation study using hCB_2R expressed in *E. coli* membranes (see SI Figure S2). AttoThio12 probe **6** performed best in terms of affinity and selectivity, displaying single-digit nanomolar hCB_2R K_i as well as 228-fold selectivity over hCB_1R. In a cAMP assay,[51] **6** displayed lower efficacy, showing a trend toward partial agonism, and exclusively activated hCB_2R over hCB_1R: hCB_2R cAMP EC_{50} = 5.6 nM, hCB_1R/hCB_2R EC_{50} ratio >1785. The weaker affinity of Alexa647 probe **4** to hCB_2R was unexpected, as it showed excellent CB_2R specificity in live-cell flow cytometry at concentrations below its apparent K_i, as discussed below. In forskolin-stimulated cAMP assay, **4** exhibited potent agonism: hCB_2R cAMP EC_{50} = 25 nM and hCB_1R/hCB_2R EC_{50} ratio = 86.

To check for interspecies differences that could compromise transferability of preclinical data from animal models to humans, binding studies were also performed with mCB_2R.[52] Probes **3a**, **3b**, **4**, and **5** showed reduced binding affinities to mCB_2R compared to hCB_2R, while **6** retained single-digit nanomolar affinity to mCB_2R, K_i = 1.1 nM. To identify potential off-targets, compound **3b** was screened against a customized panel of 50 representative proteins, including classical cannabinoid targets PPARγ and 5-HT_{1A}.[53] In this assay, **3b** exhibited very clean profile, showing only a weak interaction with prostaglandin F receptor, which was considered not relevant due to the high test concentration of 10 μM (see SI Table S2).

In summary, modular fluorophore attachment to linchpin **1** gave rise to a series of high-affinity CB_2R-selective fluorescent probes with bespoke photophysical properties. With several high-affinity and selective CB_2R fluorescent probes in hand, we set out to interrogate their utility in biological applications, with a strong focus on validation across various laboratories and cell lines.

TR-FRET-Based Determination of Equilibrium and Kinetic Binding Parameters: Radioligand-Free Assay. Radioligands are ubiquitously used to study GPCR expression as well as ligand binding affinities and kinetics.[54] Safety concerns, radioactive waste management, and, in the case of filtration assays, the need for iterative washing steps limit the applicability of radioligand-based assays for high-throughput screening (HTS). Fluorescent probes are devoid of such drawbacks and thus, in conjunction with FRET-based assays, offer attractive solutions toward the development of high-throughput equilibrium binding assays.[55−59] In addition, time-resolved methods (TR-FRET) enable studying ligand binding kinetics, one of the key determinants of drug efficacy and safety.[60−65]

Toward this end, human embryonic kidney (HEK293T-Rex) cells overexpressing SNAP-tagged hCB_2R were labeled with a SNAP-Lumi4-Tb FRET-donor (see SI). Laser excitation (337 nm) of this donor initiates energy transfer (FRET) to a proximal fluorescent probe acceptor. Membrane preparations of the derived cells were used to determine the binding kinetics of the most promising fluoroprobes, **3b** and **6**, using the TR-FRET technique by measuring the observed association rates k_{obs} at various ligand concentrations, as shown for **3b** in Figure 3A (for analogous results with **6**, see SI). The observed rates of association were found to be linearly correlated to the fluorescent probe concentration, as shown in Figure 3B for **3b**. Kinetic rate parameters k_{off} and k_{on} for the two probes were calculated by globally fitting

https://dx.doi.org/10.1021/jacs.0c05587
J. Am. Chem. Soc. 2020, 142, 16953−16964

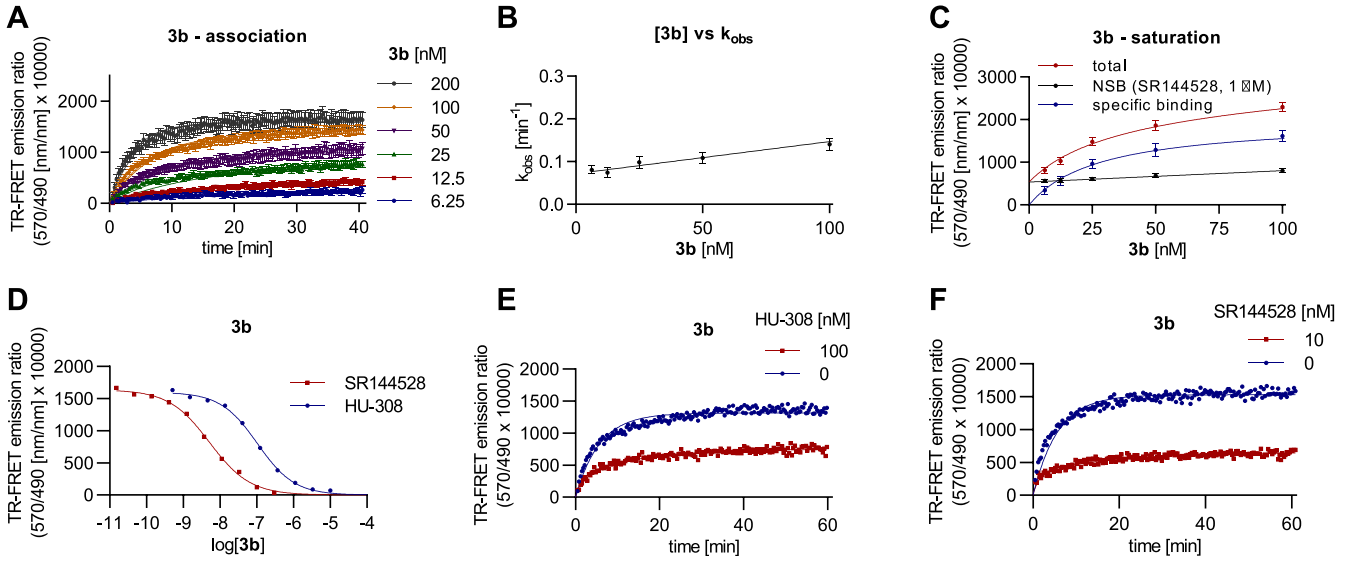

Figure 3. TR-FRET-based fluorescent probe characterization (A–C) and determination of affinities and binding kinetics of CB_2R ligands (D–F). (A) Observed association of **3b** to hCB_2R. (B) Observed association rate, k_{obs}, increases linearly with **3b** concentration. (C) Saturation analysis showing the binding of **3b** to hCB_2R. (D) Competition between **3b** (100 nM) and increasing concentrations of CB_2R-selective ligands HU-308 and SR144528 for hCB_2R. Probe **3b** competitive association curves in the presence of HU-308 (E) and SR144528 (F). Kinetic and equilibrium data were fitted to the equations described in the SI to calculate K_d, k_{on}, and k_{off} values for fluorescent and for unlabeled ligands. Data are summarized in Tables 2 and 3, and are presented as mean ± SEM, N = 3–5.

association time courses. The ratio of these parameters, k_{off}/k_{on}, is equivalent to the ligand dissociation constant K_d. Saturation binding analysis provided additional means for determining binding constants as shown for **3b** in Figure 3C. Reassuringly, the two sets of K_d values were in good agreement: 35 vs 36 nM for **3b** and 18 vs 13 nM for **6**, as shown in Table 2.

Table 2. Binding Parameters of Fluorescent Probes to hCB_2R as determined by TR-FRET[a]

compd	k_{on} [10^6 M^{-1} min^{-1}]	k_{off} [min^{-1}]	kinetic K_d [nM]	saturation K_d [nM]
3b	1.2 ± 0.1	0.04 ± 0.01	35 ± 7	36 ± 4
6	1.9 ± 0.5	0.03 ± 0.05	18 ± 3	13 ± 2

[a]Data are presented as mean ± SEM, N = 3–5.

Additionally, good correlation was found between K_i values for **3b**, **4**, and **6** determined independently by FRET and by radioligand studies. Together with microscopy data showing membrane localization of SNAP-hCB_2R, this correlation justified the use of SNAP-tagged hCB_2R for further studies (see SI Figures S4 and S5). Additional control experiments were performed in order to validate the assay. The specificity of association between **3b** and CB_2R was demonstrated by experiments employing membrane preparations of cells overexpressing SNAP-tagged β_2 adrenergic receptor (Figure S6A–C). The TR-FRET emission ratio was also completely abolished by addition of unlabeled HU-308, which highlights successful FRET between receptor and probe as well as full reversibility of tracer binding (Figure S6D).

We next set out to validate **3b** and **6** as fluorescent alternatives to radioligand tracers. Binding affinities for established CB_2R-selective agonist HU-308 and inverse agonist SR144528[66] were determined in competition experiments with fluorescent probes **3b** and **6**. Results are summarized in Table 3, with competition binding curves for HU-308 and SR144528 obtained with probe **3b** presented in Figure 3D. Of note, K_i values obtained in this manner agree with previously published benchmark values based on radioligand binding assays.[19] Furthermore, the same experimental setup also allowed for successful determination of kinetic binding parameters of HU-308 and SR144528. Data obtained with **3b** in competitive association experiments are presented in Figure 3E, F, and the observed binding parameters are summarized in Table 3. The determined kinetic rate constants are in good agreement with literature data derived using a CB_2R-selective radioligand.[54] As compared to HU-308, the higher affinity of SR144528 to hCB_2R is driven by a faster on-rate, with otherwise equivalent off-rates.

To the best of our knowledge, this work is the first study of ligand binding kinetics for CB_2R-specific ligands determined by TR-FRET. Fluorescent probes **3b** and **6** are

Table 3. Kinetic and Affinity Binding Parameters of Ligands for hCB_2R as Determined by TR-FRET[a]

	HU-308					SR144528				
probe	k_{on} [10^6 M^{-1} min^{-1}]	k_{off} [min^{-1}]	RT [min]	kinetic K_d [nM]	K_i [nM]	k_{on} [10^7 M^{-1} min^{-1}]	k_{off} [min^{-1}]	RT [min]	kinetic K_d [nM]	K_i [nM]
3b	3.43 ± 1.34	0.15 ± 0.02	6.7	55 ± 15	23 ± 5	5.17 ± 1.26	0.12 ± 0.03	8.3	2.3 ± 0.3	1.5 ± 0.4
6	2.22 ± 0.84	0.10 ± 0.02	10	53 ± 12	153 ± 24	4.11 ± 1.28	0.12 ± 0.04	8.3	3.1 ± 0.3	4.9 ± 1.2

[a]Data are presented as mean ± SEM, N = 3.

https://dx.doi.org/10.1021/jacs.0c05587
J. Am. Chem. Soc. 2020, 142, 16953–16964

attractive alternatives to radioligands for the study of binding kinetics and affinities of unlabeled ligands to hCB_2R, and they are promising for HTS applications.

CB_2R Specificity in Living CHO, Human, and Murine Cells: FACS Studies. We set out to investigate the specificity of the fluorescent probes by flow cytometry. This included CHO cells overexpressing hCB_2R, mCB_2R, or hCB_1R along with wild-type CHO cells, which were incubated with fluorescent probes at varying concentrations. Notably, no negative effect on cell viability was observed at probe concentrations up to 10 μM.

In subsequent FACS analyses, cells expressing hCB_2R or mCB_2R treated with probes **3b**, **4**, and **5** showed increased mean fluorescence intensity compared to cells expressing hCB_1R, as well as wild-type cells. Alexa488 probe **5** performed particularly well, and it specifically labeled CHO cells expressing both mCB_2R and hCB_2R over a broad concentration range of 0.12−10 μM (Figure 4A). Probe **3b** also specifically labeled cells expressing hCB_2R or mCB_2R, and the increased fluorescence signal was statistically significant at **3b** concentrations >3.33 μM ($p < 0.005$, also see SI Figure S7).[67]

Additionally, Alexa647 probe **4** showed significant increase of fluorescence intensity for cells expressing hCB_2R over a concentration range of 0.37−10 μM (see SI Figure S7). It is interesting to note that the performance of **4** in FACS is somewhat at odds with its K_i value of 2.57 μM. We speculate that two factors are responsible: (1) high fluorescence intensity of Alexa647 and (2) minimal nonspecific binding by the highly charged dye, as noted previously.[68] Nonspecific membrane binding is a major concern in commonly employed CB_2R ligands, which most often are highly lipophilic in nature. Consequently, additional experiments were performed to investigate the specificity of our fluorescent probes. In particular, we examined whether preincubation of cells with CB_2R agonist JWH133 and inverse agonist RO6851228[69] prior to FACS analysis interferes with fluoroprobe binding. Both CB_2R ligands competed with probe **3b** in a concentration-dependent fashion, supporting its high target specificity (see SI Figure S7). Similarly, they efficiently displaced Alexa488 probe **5** (Figure 4B) as well as Alexa647 probe **4** (see SI Figure S7). To the best of our knowledge, these data in flow cytometry represent the first successful ligand displacement experiments of CB_2R fluorescent probes by validated CB_2R ligands.

We subsequently set out to investigate the specificity of the fluorescent probes in a living, clinically relevant, human cell line. Probe **3b** successfully labeled activated microglial cells from 5xFAD mice. These mice recapitulate phenotypes related to Alzheimer's disease (AD) such as amyloid plaques and increased expression of mCB_2R in the CNS.[70] The use of microglia derived from CB_2R knockout (5xFAD/CB_2KO)[71] mice led to significantly weaker labeling in flow cytometry, which corroborates the CB_2R specificity of **3b** in this murine AD model (Figure 5).

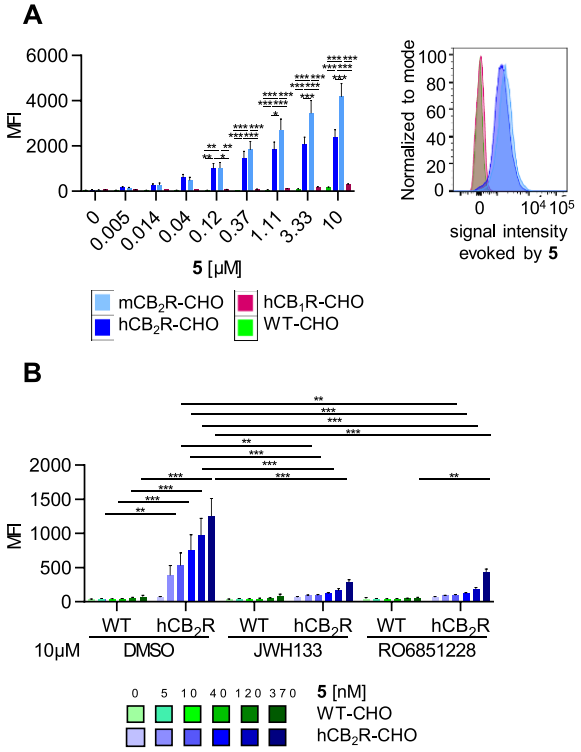

Figure 4. (A) FACS analysis of cells incubated with **5** at varying concentrations. MFI = mean fluorescence intensity. Representative fluorescence intensity histograms of cells incubated with 0.37 μM **5**. Mean ± SEM, two-way ANOVA followed by Bonferroni post hoc analysis, $*p < 0.05$; $**p < 0.01$; $***p < 0.005$, $N = 4-5$. (B) FACS analysis of cells pretreated with 10 μM of competitor ligands and subsequently stained with varying concentrations of **5**. Mean ± SEM, two-way ANOVA followed by Bonferroni post hoc analysis, $*p < 0.05$; $**p < 0.01$; $***p < 0.005$, $N = 3-5$.

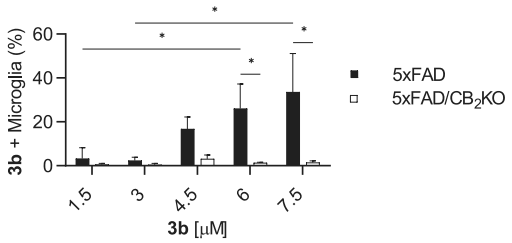

Figure 5. Fluoroprobe **3b** specifically labels mCB_2R on activated microglial cells from AD mice (5xFAD). Shown is the percentage of microglial cells positive for **3b**. $*p < 0.05$ (two-way ANOVA followed by Tukey's post hoc analysis was performed after log transformation of the fluorescence signal, $N = 4-12$).

Real-Time Receptor Visualization in Living Cells: Confocal Fluorescence Microscopy Studies. Based on the high CB_2R specificity of the fluorescent probes in FACS, the suitability of **3b** to visualize cell-surface CB_2R was assessed by real-time confocal microscopy. Exposure of CHO cells overexpressing hCB_2R to **3b** resulted in distinct time- and concentration-dependent labeling of the cell membrane. Labeling with 0.2 μM **3b** was detectable within 5 min and increased progressively over time, reaching a steady-state plateau after 8 min, and then remained unchanged, without evidence of internalization, for up to 10 min (Figure 6A, also see SI Video 1).

Of note, **3b** was only weakly fluorescent in aqueous media, allowing bright labeling of the cell membrane even in the continued presence of the probe in culture medium. As a control, at concentrations up to 0.6 μM, **3b** did not produce membrane labeling of CHO cells overexpressing hCB_1R, demonstrating the high specificity of this ligand for hCB_2R as

https://dx.doi.org/10.1021/jacs.0c05587
J. Am. Chem. Soc. 2020, 142, 16953−16964

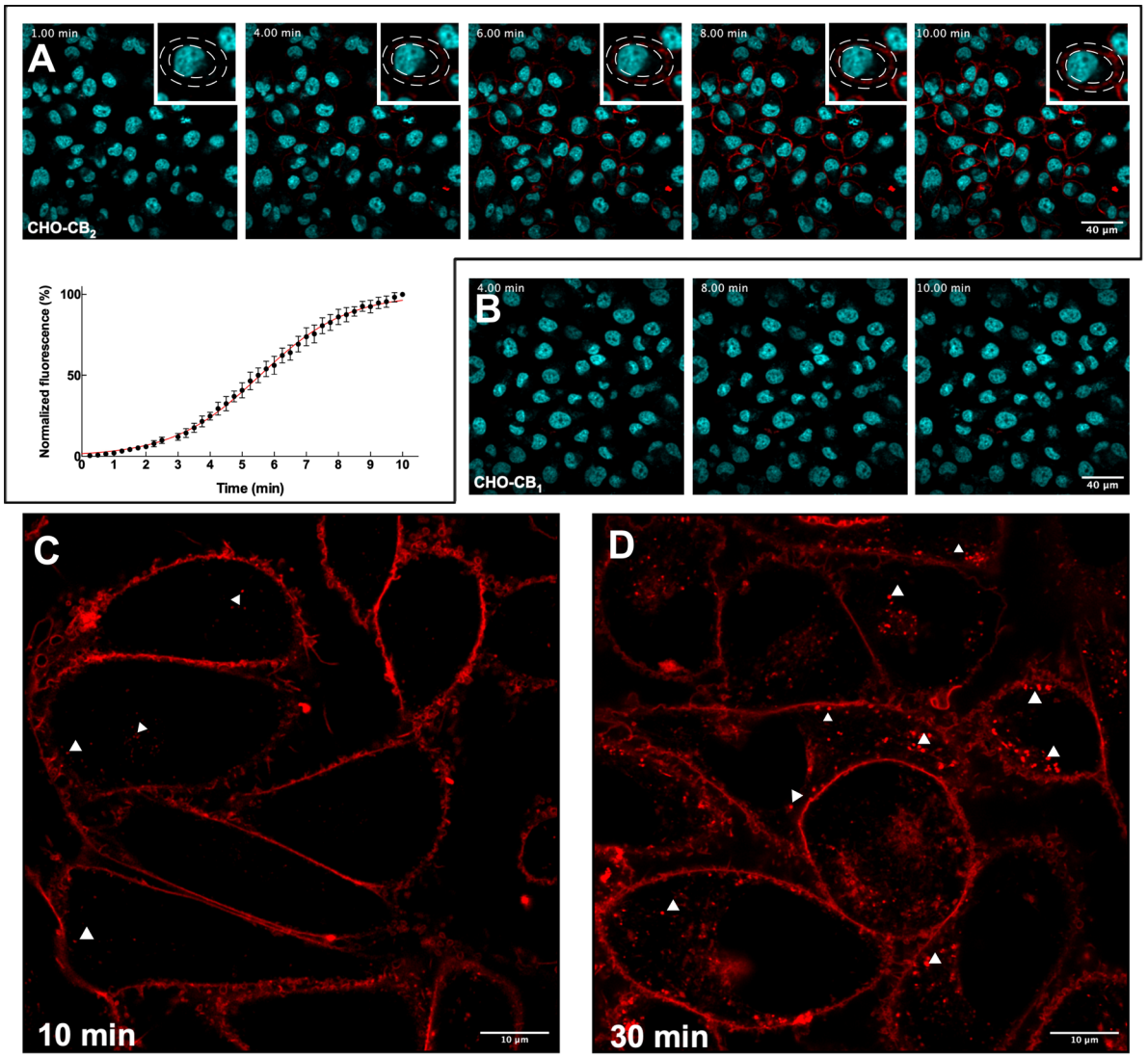

Figure 6. Confocal fluorescence microscopy with CHO cells. Different frames from time-lapse confocal microscopy of cells co-stained with **3b** (red) and Hoechst 33342 (cyan, nucleus counter stain). (A) CHO-hCB_2R cells incubated with 0.2 μM **3b** at 1, 4, 6, 8, and 10 min; at each time point, a region of interest (white strip-like curve shown in the insets) was drawn around the plasma membrane of cells (N = 6 for each field). The changes in normalized fluorescence intensity were estimated over time (Fiji software), leading to an association curve. The data on the curve represent the mean ± SD of at least three independent experiments. (B) CHO-hCB_1R cells incubated with 0.2 μM **3b** at 4, 8, and 10 min. See SI Videos 1 and 2 for animated views. Airyscan high-resolution imaging of hCB_2R-overexpressing CHO cells incubated for either (C) 10 min or (D) 30 min with 0.2 μM **3b**. Cells were optically sectioned using confocal laser-scanning microscopy equipped with an Airyscan detector. (C) In the first 10 min, **3b** staining was localized in the plasma membranes of CHO-hCB_2R cells. (D) After 30 min, brighter and increased number of vesicles, reminiscent of early endosomes, appeared below the plasma membrane and within the cytosol. Images are representative of three independent experiments.

well as its particularly low nonspecific binding (Figure 6B; also see SI Video 2).[72] Image acquisition at higher magnification and resolution was performed at the end of the recording session. After 10 min of probe administration, cell staining remained predominantly associated with the plasma membrane (Figure 6C).[73] However, after 30 min a high number of small spots was observed on the cytoplasmic side of the cell membrane as well as throughout the cytoplasm, suggesting agonist-mediated endocytosis (Figure 6D). Consistently, **3b**-induced internalization of hCB_2R was almost completely blocked in the presence of endocytosis inhibitors (see SI Figure S8). Incidentally, these findings confirmed that **3b**, which exhibited a P_{eff} of 0.4 cm/s·10^{-6} in PAMPA assay,[74] is poorly membrane-permeant.[75] Consequently, **3b** is suitable for specifically labeling hCB_2R on the cell surface for longer periods with minimal interference of agonist-mediated internalization.

Having established its suitability in cells overexpressing hCB_2R, we also investigated the potential of **3b** for primary, non-transfected cells expressing the receptor at native levels. In this context, **3b** brightly labeled mouse splenocytes (Figure 7B) and human macrophages (Figure 7E) in a time-dependent manner. In the presence of CB_2R-specific agonist JWH-133, drastic reduction of fluorescent labeling confirmed CB_2R specificity (Figure 7C,E and SI Videos 3−7). To the best of our knowledge, such specificity in living cells expressing CB_2R endogenously is unprecedented for CB_2R fluorescent probes, underscoring the (pre-)clinical promise of this probe. Collectively, these data demonstrate that DY-480XL probe **3b** is ideally suited for membrane-bound CB_2R

https://dx.doi.org/10.1021/jacs.0c05587
J. Am. Chem. Soc. 2020, 142, 16953−16964

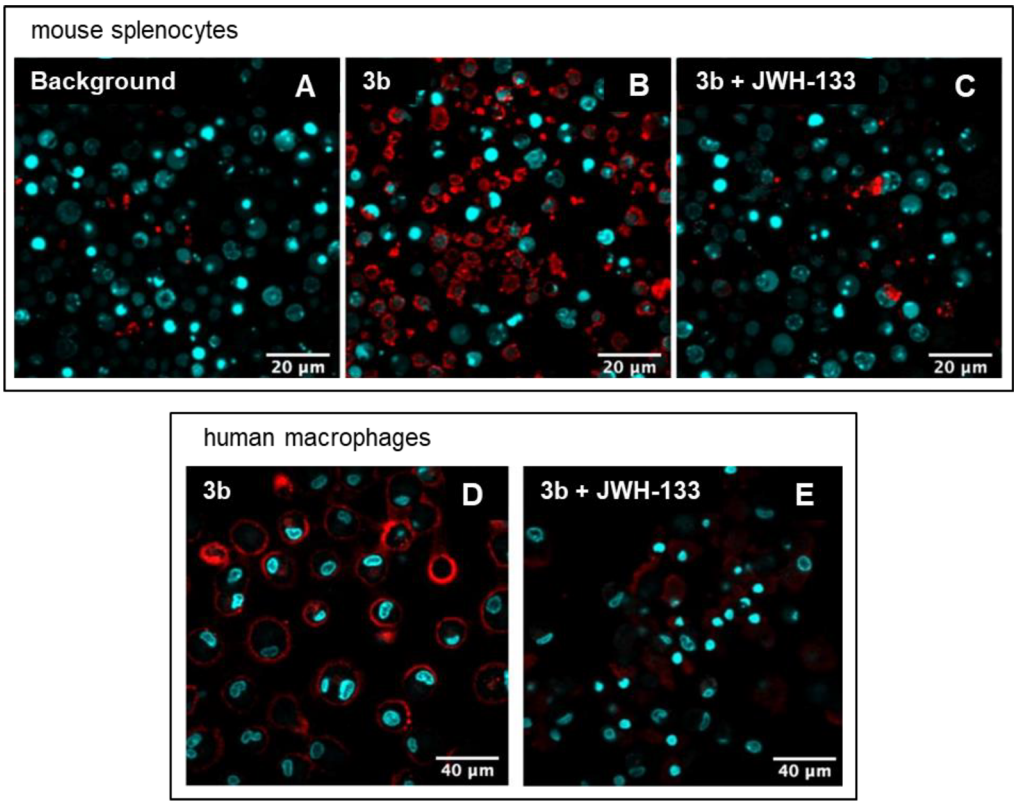

Figure 7. Confocal microscopy with primary cells expressing CB_2R endogenously. Confocal microscopy frames that show labeling of CB_2R with **3b** at 10 min in murine splenocytes and human macrophages. Murine splenocytes incubated for 10 min with (A) vehicle, (B) 0.4 μM **3b** alone, or (C) 0.4 μM **3b** in the presence of 4 μM known CB_2R agonist JWH-133 as competitor. Human macrophages for 10 min with (D) 0.6 μM **3b** alone or (E) 0.6 μM **3b** in the presence of 4 μM JWH-133. Pretreatment with Hoechst 33342 (cyan) effected nuclear counter-staining.

real-time imaging with exceedingly low levels of nonspecific binding.

CONCLUSION

A series of CB_2R-selective fluorescent probes was synthesized, characterized, and cross-validated in multiple laboratories, in order to maximize the chance for successful translation of preclinical applications. Our collaborative efforts led to identification of reliable tools for flow cytometry and time-resolved confocal microscopy with living human and murine cells expressing CB_2R. Moreover, evaluation of equilibrium and kinetic binding parameters was performed in a novel TR-FRET-based assay, which is amenable to high-throughput screening. Probes bearing DY-480XL (**3b**), Alexa488 (**5**), and AttoThio12 (**6**) dyes emerged as the most promising in terms of *in vitro* pharmacology, showing nanomolar affinity to hCB_2R and good to excellent selectivity over hCB_1R (hK_i ratios of 113, >37, and 228, respectively). Probes **3b** and **6** were used for determination of K_i values and evaluation of ligand binding kinetics of competing ligands by TR-FRET, and thus they can be used as alternatives to radioligands. Our probes allow detection and monitoring of CB_2R in cells which express the receptor endogenously, which is otherwise not possible with current antibody technology. Probes **3b**, **4**, and **5** specifically labeled mouse and human CB_2R-positive cell populations over a broad concentration range in FACS analysis. Target specificity was established by the first report of successful competition experiments with well-known CB_2R ligands (agonist and inverse agonist). Importantly, **3b** could be applied to the detection of endogenous CB_2R levels such as mCB_2R on activated AD mouse microglia. Lastly, **3b** was successfully utilized to label and monitor live cells over-expressing hCB_2R by real-time confocal fluorescence microscopy over prolonged time with minimal internalization. mCB_2R on mouse splenocytes and hCB_2R on macrophages were labeled by probe **3b**, and specificity was established by successful competition experiments with unlabeled agonist. These findings highlight the translational promise of these probes, as well as their potential for direct receptor detection, a long sought-after goal for which so far no reliable tools have been available. Consequently, **3b** is a privileged fluorescent probe for visualizing both human and murine living cells expressing CB_2R endogenously, and it may help answer fundamental questions concerning CB_2R expression in health and disease.

Considering the wealth of questions regarding CB_2R expression and function in so many different cells and tissues, it is likely that a single fluorescent probe will not meet the requirements of any given experiment. In that regard, amine platform **1** was shown to be privileged for the preparation of a collection of fluorescent ligands specifically targeting CB_2R. Hence, **1** should serve as linchpin for additional probes with bespoke pharmacological and photophysical properties. We believe the probes described herein are valuable research tools for practitioners in the field. They should find widespread use to foster better understanding of CB_2R in health and disease and to ultimately unlock the receptor's therapeutic potential.

https://dx.doi.org/10.1021/jacs.0c05587
J. Am. Chem. Soc. 2020, 142, 16953−16964

■ ASSOCIATED CONTENT

Supporting Information

The Supporting Information is available free of charge at https://pubs.acs.org/doi/10.1021/jacs.0c05587.

Supplementary figures and tables; molecular docking; in vitro pharmacology; fluorescence spectroscopy; TR-FRET kinetic CB_2R binding assay; FACS analysis; time-lapse confocal imaging; general synthetic methods; compound synthesis and characterization; NMR spectra; and N-terminal SNAP-hCB_2R sequence (PDF)

Video 1, time-lapse video of CHO-hCB_1R cells labeled with 0.2 μM **3b** for 10 min (AVI)

Video 2, time-lapse video of CHO-hCB_2R cells labeled with 0.2 μM **3b** for 10 min (AVI)

Video 3, time-lapse video of murine splenocytes incubated with 0.05% DMSO (vehicle) for 10 min to assess video background (AVI)

Video 4, time-lapse video of murine splenocytes labeled with 0.4 μM **3b** for 10 min (AVI)

Video 5, time-lapse video of murine splenocytes labeled with 0.4 μM **3b** in the presence of 4 μM JWH-133 for 10 min (AVI)

Video 6, time-lapse video of human macrophages labeled with 0.6 μM **3b** for 10 min (AVI)

Video 7, time-lapse video of human macrophages labeled with 0.6 μM **3b** in the presence of 4 μM JWH-133 for 10 min (AVI)

■ AUTHOR INFORMATION

Corresponding Authors

Erick M. Carreira − *Laboratorium für Organische Chemie, Eidgenössische Technische Hochschule Zürich, 8093 Zürich, Switzerland;* orcid.org/0000-0003-1472-490X; Email: erickm.carreira@org.chem.ethz.ch

Uwe Grether − *Roche Pharma Research & Early Development, Roche Innovation Center Basel, F. Hoffmann-La Roche Ltd., 4070 Basel, Switzerland*; Email: uwe.grether@roche.com

Authors

Roman C. Sarott − *Laboratorium für Organische Chemie, Eidgenössische Technische Hochschule Zürich, 8093 Zürich, Switzerland;* orcid.org/0000-0001-8789-6150

Matthias V. Westphal − *Laboratorium für Organische Chemie, Eidgenössische Technische Hochschule Zürich, 8093 Zürich, Switzerland*

Patrick Pfaff − *Laboratorium für Organische Chemie, Eidgenössische Technische Hochschule Zürich, 8093 Zürich, Switzerland;* orcid.org/0000-0002-9761-2497

Claudia Korn − *Roche Pharma Research & Early Development, Roche Innovation Center Basel, F. Hoffmann-La Roche Ltd., 4070 Basel, Switzerland*

David A. Sykes − *Faculty of Medicine & Health Sciences, University of Nottingham, Nottingham NG7 2UH, U.K.; Centre of Membrane Proteins and Receptors (COMPARE), University of Birmingham and University of Nottingham, Midlands B15 2TT, U.K.*

Thais Gazzi − *Leibniz-Institut für Molekulare Pharmakologie FMP, 13125 Berlin, Germany*

Benjamin Brennecke − *Leibniz-Institut für Molekulare Pharmakologie FMP, 13125 Berlin, Germany*

Kenneth Atz − *Roche Pharma Research & Early Development, Roche Innovation Center Basel, F. Hoffmann-La Roche Ltd., 4070 Basel, Switzerland*

Marie Weise − *Leibniz-Institut für Molekulare Pharmakologie FMP, 13125 Berlin, Germany*

Yelena Mostinski − *Leibniz-Institut für Molekulare Pharmakologie FMP, 13125 Berlin, Germany*

Pattarin Hompluem − *Faculty of Medicine & Health Sciences, University of Nottingham, Nottingham NG7 2UH, U.K.; Centre of Membrane Proteins and Receptors (COMPARE), University of Birmingham and University of Nottingham, Midlands B15 2TT, U.K.*

Eline Koers − *Faculty of Medicine & Health Sciences, University of Nottingham, Nottingham NG7 2UH, U.K.; Centre of Membrane Proteins and Receptors (COMPARE), University of Birmingham and University of Nottingham, Midlands B15 2TT, U.K.*

Tamara Miljuš − *Faculty of Medicine & Health Sciences, University of Nottingham, Nottingham NG7 2UH, U.K.; Centre of Membrane Proteins and Receptors (COMPARE), University of Birmingham and University of Nottingham, Midlands B15 2TT, U.K.*

Nicolas J. Roth − *William Harvey Research Institute, Barts and the London School of Medicine, Queen Mary University of London, London EC1M 6BQ, England*

Hermon Asmelash − *William Harvey Research Institute, Barts and the London School of Medicine, Queen Mary University of London, London EC1M 6BQ, England*

Man C. Vong − *Faculty of Medicine & Health Sciences, University of Nottingham, Nottingham NG7 2UH, U.K.; Centre of Membrane Proteins and Receptors (COMPARE), University of Birmingham and University of Nottingham, Midlands B15 2TT, U.K.*

Jacopo Piovesan − *Faculty of Medicine & Health Sciences, University of Nottingham, Nottingham NG7 2UH, U.K.; Centre of Membrane Proteins and Receptors (COMPARE), University of Birmingham and University of Nottingham, Midlands B15 2TT, U.K.*

Wolfgang Guba − *Roche Pharma Research & Early Development, Roche Innovation Center Basel, F. Hoffmann-La Roche Ltd., 4070 Basel, Switzerland*

Arne C. Rufer − *Roche Pharma Research & Early Development, Roche Innovation Center Basel, F. Hoffmann-La Roche Ltd., 4070 Basel, Switzerland*

Eric A. Kusznir − *Roche Pharma Research & Early Development, Roche Innovation Center Basel, F. Hoffmann-La Roche Ltd., 4070 Basel, Switzerland*

Sylwia Huber − *Roche Pharma Research & Early Development, Roche Innovation Center Basel, F. Hoffmann-La Roche Ltd., 4070 Basel, Switzerland*

Catarina Raposo − *Roche Pharma Research & Early Development, Roche Innovation Center Basel, F. Hoffmann-La Roche Ltd., 4070 Basel, Switzerland*

Elisabeth A. Zirwes − *Roche Pharma Research & Early Development, Roche Innovation Center Basel, F. Hoffmann-La Roche Ltd., 4070 Basel, Switzerland*

Anja Osterwald − *Roche Pharma Research & Early Development, Roche Innovation Center Basel, F. Hoffmann-La Roche Ltd., 4070 Basel, Switzerland*

Anto Pavlovic − *Roche Pharma Research & Early Development, Roche Innovation Center Basel, F. Hoffmann-La Roche Ltd., 4070 Basel, Switzerland*

https://dx.doi.org/10.1021/jacs.0c05587
J. Am. Chem. Soc. 2020, 142, 16953−16964

Svenja Moes − *Roche Pharma Research & Early Development, Roche Innovation Center Basel, F. Hoffmann-La Roche Ltd., 4070 Basel, Switzerland*
Jennifer Beck − *Roche Pharma Research & Early Development, Roche Innovation Center Basel, F. Hoffmann-La Roche Ltd., 4070 Basel, Switzerland*
Irene Benito-Cuesta − *Faculty of Experimental Sciences, Universidad Francisco de Vitoria, 28223 Madrid, Spain*
Teresa Grande − *Faculty of Experimental Sciences, Universidad Francisco de Vitoria, 28223 Madrid, Spain*
Samuel Ruiz de Martín Esteban − *Faculty of Experimental Sciences, Universidad Francisco de Vitoria, 28223 Madrid, Spain*
Alexei Yeliseev − *National Institute on Alcohol Abuse and Alcoholism, National Institutes of Health, Rockville, Maryland 20852, United States*
Faye Drawnel − *Roche Pharma Research & Early Development, Roche Innovation Center Basel, F. Hoffmann-La Roche Ltd., 4070 Basel, Switzerland*
Gabriella Widmer − *Roche Pharma Research & Early Development, Roche Innovation Center Basel, F. Hoffmann-La Roche Ltd., 4070 Basel, Switzerland*
Daniela Holzer − *Roche Pharma Research & Early Development, Roche Innovation Center Basel, F. Hoffmann-La Roche Ltd., 4070 Basel, Switzerland*
Tom van der Wel − *Department of Molecular Physiology, Leiden Institute of Chemistry, Leiden University, 2333 CC Leiden, The Netherlands*
Harpreet Mandhair − *Institute of Biochemistry and Molecular Medicine, University of Bern, 3012 Bern, Switzerland*
Cheng-Yin Yuan − *Department of Microbiology and Immunology, Neuroscience Research Center, Medical College of Wisconsin, Milwaukee, Wisconsin 53226, United States*
William R. Drobyski − *Department of Medicine, Neuroscience Research Center, Medical College of Wisconsin, Milwaukee, Wisconsin 53226, United States*
Yurii Saroz − *Department of Pharmacology and Clinical Pharmacology, School of Medical Sciences, Faculty of Medical and Health Sciences, University of Auckland, 1142 Auckland, New Zealand*
Natasha Grimsey − *Department of Pharmacology and Clinical Pharmacology, School of Medical Sciences, Faculty of Medical and Health Sciences, University of Auckland, 1142 Auckland, New Zealand;* orcid.org/0000-0003-3941-4537
Michael Honer − *Roche Pharma Research & Early Development, Roche Innovation Center Basel, F. Hoffmann-La Roche Ltd., 4070 Basel, Switzerland*
Jürgen Fingerle − *Roche Pharma Research & Early Development, Roche Innovation Center Basel, F. Hoffmann-La Roche Ltd., 4070 Basel, Switzerland*
Klaus Gawrisch − *National Institute on Alcohol Abuse and Alcoholism, National Institutes of Health, Rockville, Maryland 20852, United States*
Julian Romero − *Faculty of Experimental Sciences, Universidad Francisco de Vitoria, 28223 Madrid, Spain*
Cecilia J. Hillard − *Department of Pharmacology and Clinical Pharmacology, Neuroscience Research Center, Medical College of Wisconsin, Milwaukee, Wisconsin 53226, United States*
Zoltan V. Varga − *National Institute on Alcohol Abuse and Alcoholism, National Institutes of Health, Rockville, Maryland 20852, United States; HCEMM-SU Cardiometabolic Immunology Research Group, Department of Pharmacology and Pharmacotherapy, Semmelweis University, 1085 Budapest, Hungary*
Mario van der Stelt − *Department of Molecular Physiology, Leiden Institute of Chemistry, Leiden University, 2333 CC Leiden, The Netherlands;* orcid.org/0000-0002-1029-5717
Pal Pacher − *National Institute on Alcohol Abuse and Alcoholism, National Institutes of Health, Rockville, Maryland 20852, United States*
Jürg Gertsch − *Institute of Biochemistry and Molecular Medicine, University of Bern, 3012 Bern, Switzerland*
Peter J. McCormick − *William Harvey Research Institute, Barts and the London School of Medicine, Queen Mary University of London, London EC1M 6BQ, England*
Christoph Ullmer − *Roche Pharma Research & Early Development, Roche Innovation Center Basel, F. Hoffmann-La Roche Ltd., 4070 Basel, Switzerland*
Sergio Oddi − *Faculty of Veterinary Medicine, University of Teramo, 64100 Teramo, Italy; European Center for Brain Research (CERC)/Santa Lucia Foundation, 00179 Rome, Italy*
Mauro Maccarrone − *European Center for Brain Research (CERC)/Santa Lucia Foundation, 00179 Rome, Italy; Department of Applied Clinical and Biotechnological Sciences, University of L'Aquila, 67100 L'Aquila, Italy*
Dmitry B. Veprintsev − *Faculty of Medicine & Health Sciences, University of Nottingham, Nottingham NG7 2UH, U.K.; Centre of Membrane Proteins and Receptors (COMPARE), University of Birmingham and University of Nottingham, Midlands B15 2TT, U.K.;* orcid.org/0000-0002-3583-5409
Marc Nazaré − *Leibniz-Institut für Molekulare Pharmakologie FMP, 13125 Berlin, Germany;* orcid.org/0000-0002-1602-2330

Complete contact information is available at: https://pubs.acs.org/10.1021/jacs.0c05587

Notes

The authors declare no competing financial interest.

■ ACKNOWLEDGMENTS

E.M.C. is grateful to ETH Zürich and F. Hoffmann-La Roche for support of the research program. R.C.S. and P.P. acknowledge a fellowship by the Scholarship Fund of the Swiss Chemical Industry (SSCI). M.M. and S.O. thank Dr. Lucia Scipioni and Dr. Antonio Totaro for cell culture and technical support, and Dr. Daunia Laurenti for technical assistance in live imaging. They are also grateful to the Italian Ministry of Education, University and Research (MIUR) for partial financial support under the competitive grant PRIN 2015. J.R. acknowledges a grant by Ministerio de Economía y Competitividad (SAF 2016-75959-R). P.J.M. thanks the QMUL MRC-DTP for funding for N.J.R. Björn Wagner, Virginie Micallef, and Joelle Muller are acknowledged for the generation of PAMPA data. Some aspects of developing TR-FRET assay were supported by Swiss National Science Foundation grant 159748 to D.B.V.

■ REFERENCES

(1) Marzo, V. D.; Bifulco, M.; Petrocellis, L. D. The Endocannabinoid System and Its Therapeutic Exploitation. *Nat. Rev. Drug Discovery* **2004**, *3*, 771.

(2) Matsuda, L. A.; Lolait, S. J.; Brownstein, M. J.; Young, A. C.; Bonner, T. I. Structure of a Cannabinoid Receptor and Functional Expression of the Cloned CDNA. *Nature* **1990**, *346*, 561.
(3) Munro, S.; Thomas, K. L.; Abu-Shaar, M. Molecular Characterization of a Peripheral Receptor for Cannabinoids. *Nature* **1993**, *365*, 61.
(4) Maccarrone, M.; Bab, I.; Bíró, T.; Cabral, G. A.; Dey, S. K.; Di Marzo, V.; Konje, J. C.; Kunos, G.; Mechoulam, R.; Pacher, P.; Sharkey, K. A.; Zimmer, A. Endocannabinoid Signaling at the Periphery: 50 Years after THC. *Trends Pharmacol. Sci.* **2015**, *36*, 277.
(5) Izzo, A. A.; Borrelli, F.; Capasso, R.; Di Marzo, V.; Mechoulam, R. Non-Psychotropic Plant Cannabinoids: New Therapeutic Opportunities from an Ancient Herb. *Trends Pharmacol. Sci.* **2009**, *30*, 515.
(6) Galiègue, S.; Mary, S.; Marchand, J.; Dussossoy, D.; Carrière, D.; Carayon, P.; Bouaboula, M.; Shire, D.; Le Fur, G.; Casellas, P. Expression of Central and Peripheral Cannabinoid Receptors in Human Immune Tissues and Leukocyte Subpopulations. *Eur. J. Biochem.* **1995**, *232*, 54.
(7) Turcotte, C.; Blanchet, M.-R.; Laviolette, M.; Flamand, N. The CB2 Receptor and Its Role as a Regulator of Inflammation. *Cell. Mol. Life Sci.* **2016**, *73*, 4449.
(8) Pacher, P.; Mechoulam, R. Is Lipid Signaling through Cannabinoid 2 Receptors Part of a Protective System? *Prog. Lipid Res.* **2011**, *50*, 193.
(9) Guindon, J.; Hohmann, A. G. Cannabinoid CB2 Receptors: A Therapeutic Target for the Treatment of Inflammatory and Neuropathic Pain. *Br. J. Pharmacol.* **2008**, *153*, 319.
(10) Pacher, P.; Kunos, G. Modulating the Endocannabinoid System in Human Health and Disease–Successes and Failures. *FEBS J.* **2013**, *280*, 1918.
(11) Dhopeshwarkar, A.; Mackie, K. CB2 Cannabinoid Receptors as a Therapeutic Target—What Does the Future Hold? *Mol. Pharmacol.* **2014**, *86*, 430.
(12) Han, S.; Thatte, J.; Buzard, D. J.; Jones, R. M. Therapeutic Utility of Cannabinoid Receptor Type 2 (CB2) Selective Agonists. *J. Med. Chem.* **2013**, *56*, 8224.
(13) Marchalant, Y.; Brownjohn, P. W.; Bonnet, A.; Kleffmann, T.; Ashton, J. C. Validating Antibodies to the Cannabinoid CB2 Receptor: Antibody Sensitivity Is Not Evidence of Antibody Specificity. *J. Histochem. Cytochem.* **2014**, *62*, 395.
(14) Zhang, H.-Y.; Shen, H.; Jordan, C. J.; Liu, Q.-R.; Gardner, E. L.; Bonci, A.; Xi, Z.-X. CB2 Receptor Antibody Signal Specificity: Correlations with the Use of Partial CB2-Knockout Mice and Anti-Rat CB2 Receptor Antibodies. *Acta Pharmacol. Sin.* **2019**, *40*, 398–409.
(15) Cécyre, B.; Thomas, S.; Ptito, M.; Casanova, C.; Bouchard, J.-F. Evaluation of the Specificity of Antibodies Raised against Cannabinoid Receptor Type 2 in the Mouse Retina. *Naunyn-Schmiedeberg's Arch. Pharmacol.* **2014**, *387*, 17.
(16) Cabral, G. A.; Marciano-Cabral, F. Cannabinoid Receptors in Microglia of the Central Nervous System: Immune Functional Relevance. *J. Leukocyte Biol.* **2005**, *78*, 1192.
(17) Ashton, J. C.; Glass, M. The Cannabinoid CB2 Receptor as a Target for Inflammation-Dependent Neurodegeneration. *Curr. Neuropharmacol.* **2007**, *5*, 73.
(18) Grimsey, N. L.; Goodfellow, C. E.; Dragunow, M.; Glass, M. Cannabinoid Receptor 2 Undergoes Rab5-Mediated Internalization and Recycles via a Rab11-Dependent Pathway. *Biochim. Biophys. Acta, Mol. Cell Res.* **2011**, *1813*, 1554.
(19) Soethoudt, M.; Grether, U.; Fingerle, J.; Grim, T. W.; Fezza, F.; de Petrocellis, L.; Ullmer, C.; Rothenhausler, B.; Perret, C.; van Gils, N.; Finlay, D.; MacDonald, C.; Chicca, A.; Gens, M. D.; Stuart, J.; de Vries, H.; Mastrangelo, N.; Xia, L.; Alachouzos, G.; Baggelaar, M. P.; Martella, A.; Mock, E. D.; Deng, H.; Heitman, L. H.; Connor, M.; Di Marzo, V.; Gertsch, J.; Lichtman, A. H.; Maccarrone, M.; Pacher, P.; Glass, M.; van der Stelt, M. Cannabinoid CB_2 Receptor Ligand Profiling Reveals Biased Signalling and off-Target Activity. *Nat. Commun.* **2017**, *8*, 13958.
(20) Stoddart, L. A.; Kilpatrick, L. E.; Briddon, S. J.; Hill, S. J. Probing the Pharmacology of G Protein-Coupled Receptors with Fluorescent Ligands. *Neuropharmacology* **2015**, *98*, 48.
(21) Vernall, A. J.; Hill, S. J.; Kellam, B. The Evolving Small-Molecule Fluorescent-Conjugate Toolbox for Class A GPCRs. *Br. J. Pharmacol.* **2014**, *171*, 1073.
(22) Iliopoulos-Tsoutsouvas, C.; Kulkarni, R. N.; Makriyannis, A.; Nikas, S. P. Fluorescent Probes for G-Protein-Coupled Receptor Drug Discovery. *Expert Opin. Drug Discovery* **2018**, *13*, 933.
(23) Bai, M.; Sexton, M.; Stella, N.; Bornhop, D. J. MBC94, a Conjugable Ligand for Cannabinoid CB2 Receptor Imaging. *Bioconjugate Chem.* **2008**, *19*, 988.
(24) Sexton, M.; Woodruff, G.; Horne, E. A.; Lin, Y. H.; Muccioli, G. G.; Bai, M.; Stern, E.; Bornhop, D. J.; Stella, N. NIR-Mbc94, a Fluorescent Ligand That Binds to Endogenous CB2 Receptors and Is Amenable to High-Throughput Screening. *Chem. Biol.* **2011**, *18*, 563.
(25) Petrov, R. R.; Ferrini, M. E.; Jaffar, Z.; Thompson, C. M.; Roberts, K.; Diaz, P. Design and Evaluation of a Novel Fluorescent CB2 Ligand as Probe for Receptor Visualization in Immune Cells. *Bioorg. Med. Chem. Lett.* **2011**, *21*, 5859.
(26) Martín-Couce, L.; Martín-Fontecha, M.; Capolicchio, S.; López-Rodríguez, M. L.; Ortega-Gutiérrez, S. Development of Endocannabinoid-Based Chemical Probes for the Study of Cannabinoid Receptors. *J. Med. Chem.* **2011**, *54*, 5265.
(27) Zhang, S.; Shao, P.; Bai, M. In Vivo Type 2 Cannabinoid Receptor-Targeted Tumor Optical Imaging Using a Near Infrared Fluorescent Probe. *Bioconjugate Chem.* **2013**, *24*, 1907.
(28) Wu, Z.; Shao, P.; Zhang, S.; Bai, M. Targeted Zwitterionic near Infrared Fluorescent Probe for Improved Imaging of Type 2 Cannabinoid Receptors. *J. Biomed. Opt.* **2014**, *19*, 036006.
(29) Zhang, S.; Jia, N.; Shao, P.; Tong, Q.; Xie, X.-Q.; Bai, M. Target-Selective Phototherapy Using a Ligand-Based Photosensitizer for Type 2 Cannabinoid Receptor. *Chem. Biol.* **2014**, *21*, 338.
(30) Ling, X.; Zhang, S.; Shao, P.; Li, W.; Yang, L.; Ding, Y.; Xu, C.; Stella, N.; Bai, M. A Novel Near-Infrared Fluorescence Imaging Probe That Preferentially Binds to Cannabinoid Receptors CB_2R over CB_1R. *Biomaterials* **2015**, *57*, 169.
(31) Zubiaurre, A. R. Chemical Probes for the Study of the Endogenous Cannabinoid System (Doctoral dissertation) Universidad Complutense de Madrid, Spain, 2016.
(32) Cooper, A. G.; Oyagawa, C. R. M.; Manning, J. J.; Singh, S.; Hook, S.; Grimsey, N. L.; Glass, M.; Tyndall, J. D. A.; Vernall, A. J. Development of Selective, Fluorescent Cannabinoid Type 2 Receptor Ligands Based on a 1,8-Naphthyridin-2-(1H)-One-3-Carboxamide Scaffold. *MedChemComm* **2018**, *9*, 2055.
(33) Cooper, A. G.; MacDonald, C.; Glass, M.; Hook, S.; Tyndall, J. D. A.; Vernall, A. J. Alkyl Indole-Based Cannabinoid Type 2 Receptor Tools: Exploration of Linker and Fluorophore Attachment. *Eur. J. Med. Chem.* **2018**, *145*, 770.
(34) Spinelli, F.; Giampietro, R.; Stefanachi, A.; Riganti, C.; Kopecka, J.; Abatematteo, F. S.; Leonetti, F.; Colabufo, N. A.; Mangiatordi, G. F.; Nicolotti, O.; Perrone, M. G.; Brea, J.; Loza, M. I.; Infantino, V.; Abate, C.; Contino, M. Design and Synthesis of Fluorescent Ligands for the Detection of Cannabinoid Type 2 Receptor (CB_2R). *Eur. J. Med. Chem.* **2020**, *188*, 112037.
(35) Singh, S.; Oyagawa, C. R. M.; Macdonald, C.; Grimsey, N. L.; Glass, M.; Vernall, A. J. Chromenopyrazole-Based High Affinity, Selective Fluorescent Ligands for Cannabinoid Type 2 Receptor. *ACS Med. Chem. Lett.* **2019**, *10*, 209.
(36) Martín-Couce, L.; Martín-Fontecha, M.; Palomares, Ó.; Mestre, L.; Cordomí, A.; Hernangomez, M.; Palma, S.; Pardo, L.; Guaza, C.; López-Rodríguez, M. L.; Ortega-Gutiérrez, S. Chemical Probes for the Recognition of Cannabinoid Receptors in Native Systems. *Angew. Chem., Int. Ed.* **2012**, *51*, 6896.
(37) Soethoudt, M.; Stolze, S. C.; Westphal, M. V.; van Stralen, L.; Martella, A.; van Rooden, E. J.; Guba, W.; Varga, Z. V.; Deng, H.;

https://dx.doi.org/10.1021/jacs.0c05587
J. Am. Chem. Soc. 2020, 142, 16953–16964

van Kasteren, S. I.; Grether, U.; IJzerman, A. P.; Pacher, P.; Carreira, E. M.; Overkleeft, H. S.; Ioan-Facsinay, A.; Heitman, L. H.; van der Stelt, M. Selective Photoaffinity Probe That Enables Assessment of Cannabinoid CB_2 Receptor Expression and Ligand Engagement in Human Cells. *J. Am. Chem. Soc.* **2018**, *140*, 6067.
(38) Hanuš, L.; Breuer, A.; Tchilibon, S.; Shiloah, S.; Goldenberg, D.; Horowitz, M.; Pertwee, R. G.; Ross, R. A.; Mechoulam, R.; Fride, E. HU-308: A Specific Agonist for CB2, a Peripheral Cannabinoid Receptor. *Proc. Natl. Acad. Sci. U. S. A.* **1999**, *96*, 14228.
(39) Westphal, M. V.; Sarott, R. C.; Zirwes, E. A.; Osterwald, A.; Guba, W.; Ullmer, C.; Grether, U.; Carreira, E. M. Highly Selective, Amine-Derived Cannabinoid Receptor 2 Probes. *Chem. - Eur. J.* **2020**, *26*, 1380.
(40) Ma, Z.; Du, L.; Li, M. Toward Fluorescent Probes for G-Protein-Coupled Receptors (GPCRs). *J. Med. Chem.* **2014**, *57*, 8187.
(41) Leopoldo, M.; Lacivita, E.; Berardi, F.; Perrone, R. Developments in Fluorescent Probes for Receptor Research. *Drug Discovery Today* **2009**, *14*, 706.
(42) Mazères, S.; Schram, V.; Tocanne, J. F.; Lopez, A. 7-Nitrobenz-2-Oxa-1,3-Diazole-4-Yl-Labeled Phospholipids in Lipid Membranes: Differences in Fluorescence Behavior. *Biophys. J.* **1996**, *71*, 327.
(43) Comerci, C. J.; Herrmann, J.; Yoon, J.; Jabbarpour, F.; Zhou, X.; Nomellini, J. F.; Smit, J.; Shapiro, L.; Wakatsuki, S.; Moerner, W. E. Topologically-Guided Continuous Protein Crystallization Controls Bacterial Surface Layer Self-Assembly. *Nat. Commun.* **2019**, *10*, 2731.
(44) Berlier, J. E.; Rothe, A.; Buller, G.; Bradford, J.; Gray, D. R.; Filanoski, B. J.; Telford, W. G.; Yue, S.; Liu, J.; Cheung, C.-Y.; Chang, W.; Hirsch, J. D.; Beechem, R. P.; Haugland, J. M.; Haugland, R. P. Quantitative Comparison of Long-Wavelength Alexa Fluor Dyes to Cy Dyes: Fluorescence of the Dyes and Their Bioconjugates. *J. Histochem. Cytochem.* **2003**, *51*, 1699.
(45) Lindhoud, S.; Westphal, A. H.; Visser, A. J. W. G.; Borst, J. W.; van Mierlo, C. P. M. Fluorescence of Alexa Fluor Dye Tracks Protein Folding. *PLoS One* **2012**, *7*, e46838.
(46) Chmyrov, A.; Arden-Jacob, J.; Zilles, A.; Drexhage, K.-H.; Widengren, J. Characterization of New Fluorescent Labels for Ultra-High Resolution Microscopy. *Photochem. Photobiol. Sci.* **2008**, *7*, 1378.
(47) The increased affinity of **6** compared to **3b** is surprising given their structural similarity. It is well known that ligand−membrane interactions can lead to increased local ligand concentration, leading to increased affinity in binding assays. We hypothesize that this may be the reason for the K_i difference between probes **6** and **3b**: (a) Gherbi, K.; Briddon, S. J.; Charlton, S. J. Micro-Pharmacokinetics: Quantifying Local Drug Concentration at Live Cell Membranes. *Sci. Rep.* **2018**, *8*, 3479. (b) Zumbuehl, A.; Stano, P.; Sohrmann, M.; Dietiker, R.; Peter, M.; Carreira, E. M. Synthesis and Investigation of Tryptophan−Amphotericin B Conjugates. *ChemBioChem* **2009**, *10*, 1617.
(48) Li, X.; Hua, T.; Vemuri, K.; Ho, J.-H.; Wu, Y.; Wu, L.; Popov, P.; Benchama, O.; Zvonok, N.; Locke, K.; Qu, L.; Han, G. W.; Iyer, M. R.; Cinar, R.; Coffey, N. J.; Wang, J.; Wu, M.; Katritch, V.; Zhao, S.; Kunos, G.; Bohn, L. M.; Makriyannis, A.; Stevens, R. C.; Liu, Z.-J. Crystal Structure of the Human Cannabinoid Receptor CB_2. *Cell* **2019**, *176*, 459.
(49) Xing, C.; Zhuang, Y.; Xu, T.-H.; Feng, Z.; Zhou, X. E.; Chen, M.; Wang, L.; Meng, X.; Xue, Y.; Wang, J.; Liu, H.; McGuire, T. F.; Zhao, G.; Melcher, K.; Zhang, C.; Xu, H. E.; Xie, X.-Q. Cryo-EM Structure of the Human Cannabinoid Receptor CB_2-G_i Signaling Complex. *Cell* **2020**, *180*, 645.
(50) Hua, T.; Li, X.; Wu, L.; Iliopoulos-Tsoutsouvas, C.; Wang, Y.; Wu, M.; Shen, L.; Johnston, C. A.; Nikas, S. P.; Song, F.; Song, X.; Yuan, S.; Sun, Q.; Wu, Y.; Jiang, S.; Grim, T. W.; Benchama, O.; Stahl, E. L.; Zvonok, N.; Zhao, S.; Bohn, L. M.; Makriyannis, A.; Liu, Z.-J. Activation and Signaling Mechanism Revealed by Cannabinoid Receptor-Gi Complex Structures. *Cell* **2020**, *180*, 655.
(51) CBRs inhibit adenylyl cyclase via $G_{\alpha i}$ subunits, and activation decreases cellular cAMP. We measured the effect of our probes on forskolin-stimulated cAMP generation by endogenous adenylyl cyclase using a time-resolved FRET-based assay (PerkinElmer).
(52) Unfortunately, our consortium does not have a mCB_1R binding assay in place. Consequently, we were not able to generate murine receptor selectivity (mCB_2R vs mCB_1R) data. However, the amino acid sequences of hCB_1R and mCB1R binding pockets only differ in one residue, Ile105 (h) as opposed to Met (m). For probes showing good selectivity for hCB_2R, similar selectivity can be expected also for murine receptors. Liu, Q.-R.; Pan, C.-H.; Hishimoto, A.; Li, C.-Y.; Xi, Z.-X.; Llorente-Berzal, A.; Viveros, M.-P.; Ishiguro, H.; Arinami, T.; Onaivi, E. S.; Uhl, G. R. Species Differences in Cannabinoid Receptor 2 (CNR2 Gene): Identification of Novel Human and Rodent CB2 Isoforms, Differential Tissue Expression, and Regulation by Cannabinoid Receptor Ligands. *Genes, Brain Behav.* **2009**, *8*, 519.
(53) Bendels, S.; Bissantz, C.; Fasching, B.; Gerebtzoff, G.; Guba, W.; Kansy, M.; Migeon, J.; Mohr, S.; Peters, J.-U.; Tillier, F.; Wyler, R.; Lerner, C.; Kramer, C.; Richter, H.; Roberts, S. Safety Screening in Early Drug Discovery: An Optimized Assay Panel. *J. Pharmacol. Toxicol. Methods* **2019**, *99*, 106609.
(54) Martella, A.; Sijben, H.; Rufer, A. C.; Grether, U.; Fingerle, J.; Ullmer, C.; Hartung, T.; IJzerman, A. P.; van der Stelt, M.; Heitman, L. H. A Novel Selective Inverse Agonist of the CB_2 Receptor as a Radiolabeled Tool Compound for Kinetic Binding Studies. *Mol. Pharmacol.* **2017**, *92*, 389.
(55) Albizu, L.; Teppaz, G.; Seyer, R.; Bazin, H.; Ansanay, H.; Manning, M.; Mouillac, B.; Durroux, T. Toward Efficient Drug Screening by Homogeneous Assays Based on the Development of New Fluorescent Vasopressin and Oxytocin Receptor Ligands. *J. Med. Chem.* **2007**, *50*, 4976.
(56) Loison, S.; Cottet, M.; Orcel, H.; Adihou, H.; Rahmeh, R.; Lamarque, L.; Trinquet, E.; Kellenberger, E.; Hibert, M.; Durroux, T.; Mouillac, B.; Bonnet, D. Selective Fluorescent Nonpeptidic Antagonists For Vasopressin V2 GPCR: Application To Ligand Screening and Oligomerization Assays. *J. Med. Chem.* **2012**, *55*, 8588.
(57) Zwier, J. M.; Roux, T.; Cottet, M.; Durroux, T.; Douzon, S.; Bdioui, S.; Gregor, N.; Bourrier, E.; Oueslati, N.; Nicolas, L.; Tinel, N.; Boisseau, C.; Yverneau, P.; Charrier-Savournin, F.; Fink, M.; Trinquet, E. A Fluorescent Ligand-Binding Alternative Using Tag-Lite® Technology. *J. Biomol. Screening* **2010**, *15*, 1248.
(58) Leyris, J.-P.; Roux, T.; Trinquet, E.; Verdié, P.; Fehrentz, J.-A.; Oueslati, N.; Douzon, S.; Bourrier, E.; Lamarque, L.; Gagne, D.; Galleyrand, J.-C.; M'kadmi, C.; Martinez, J.; Mary, S.; Banères, J.-L.; Marie, J. Homogeneous Time-Resolved Fluorescence-Based Assay to Screen for Ligands Targeting the Growth Hormone Secretagogue Receptor Type 1a. *Anal. Biochem.* **2011**, *408* (2), 253−262.
(59) Martinez-Pinilla, E.; Rabal, O.; Reyes-Resina, I.; Zamarbide, M.; Navarro, G.; Sanchez-Arias, J. A.; de Miguel, I.; Lanciego, J. L.; Oyarzabal, J.; Franco, R. Two Affinity Sites of the Cannabinoid Subtype 2 Receptor Identified by a Novel Homogeneous Binding Assay. *J. Pharmacol. Exp. Ther.* **2016**, *358*, 580.
(60) Copeland, R. A.; Pompliano, D. L.; Meek, T. D. Drug−Target Residence Time and Its Implications for Lead Optimization. *Nat. Rev. Drug Discovery* **2006**, *5*, 730.
(61) Swinney, D. C. The Role of Binding Kinetics in Therapeutically Useful Drug Action. *Curr. Opin. Drug Discovery Devel.* **2009**, *12*, 31.
(62) Lu, H.; Tonge, P. J. Drug-Target Residence Time: Critical Information for Lead Optimization. *Curr. Opin. Chem. Biol.* **2010**, *14*, 467.
(63) Lane, J. R.; May, L. T.; Parton, R. G.; Sexton, P. M.; Christopoulos, A. A Kinetic View of GPCR Allostery and Biased Agonism. *Nat. Chem. Biol.* **2017**, *13*, 929.
(64) Klein Herenbrink, C.; Sykes, D. A.; Donthamsetti, P.; Canals, M.; Coudrat, T.; Shonberg, J.; Scammells, P. J.; Capuano, B.; Sexton, P. M.; Charlton, S. J.; Javitch, J. A.; Christopoulos, A.; Lane,

https://dx.doi.org/10.1021/jacs.0c05587
J. Am. Chem. Soc. 2020, 142, 16953−16964

J. R. The Role of Kinetic Context in Apparent Biased Agonism at GPCRs. *Nat. Commun.* **2016**, *7*, 10842.
(65) van der Velden, W. J. C.; Heitman, L. H.; Rosenkilde, M. M. Perspective: Implications of Ligand−Receptor Binding Kinetics for Therapeutic Targeting of G Protein-Coupled Receptors. *ACS Pharmacol. Transl. Sci.* **2020**, *3*, 179.
(66) Rinaldi-Carmona, M.; Barth, F.; Millan, J.; Derocq, J.-M.; Casellas, P.; Congy, C.; Oustric, D.; Sarran, M.; Bouaboula, M.; Calandra, B.; Portier, M.; Shire, D.; Brelière, J.-C.; Fur, G. L. SR 144528, the First Potent and Selective Antagonist of the CB_2 Cannabinoid Receptor. *J. Pharmacol. Exp. Ther.* **1998**, *284*, 644.
(67) In contrast to its corresponding K_i values, **3b** binds preferentially to mCB_2R over hCB_2R. Binding data is generated from previously frozen membranes, while FACS experiments are performed with viable cells. We hypothesize that membrane lysate preparation affects mouse and human CB_2R structure differentially, with detrimental effects on binding of **3b** to mCB_2R. In cAMP assay, which is also performed on living cells, the behavior of **3b** is similar to that in the FACS assay.
(68) Bosch, P. J.; Corrêa, I. R.; Sonntag, M. H.; Ibach, J.; Brunsveld, L.; Kanger, J. S.; Subramaniam, V. Evaluation of Fluorophores to Label SNAP-Tag Fused Proteins for Multicolor Single-Molecule Tracking Microscopy in Live Cells. *Biophys. J.* **2014**, *107*, 803.
(69) Ouali Alami, N.; Schurr, C.; Olde Heuvel, F.; Tang, L.; Li, Q.; Tasdogan, A.; Kimbara, A.; Nettekoven, M.; Ottaviani, G.; Raposo, C.; Röver, S.; Rogers-Evans, M.; Rothenhäusler, B.; Ullmer, C.; Fingerle, J.; Grether, U.; Knuesel, I.; Boeckers, T. M.; Ludolph, A.; Wirth, T.; Roselli, F.; Baumann, B. NF-KB Activation in Astrocytes Drives a Stage-Specific Beneficial Neuroimmunological Response in ALS. *EMBO J.* **2018**, *37*, e98697.
(70) Oakley, H.; Cole, S. L.; Logan, S.; Maus, E.; Shao, P.; Craft, J.; Guillozet-Bongaarts, A.; Ohno, M.; Disterhoft, J.; Van Eldik, L.; Berry, R.; Vassar, R. Intraneuronal β-Amyloid Aggregates, Neurodegeneration, and Neuron Loss in Transgenic Mice with Five Familial Alzheimer's Disease Mutations: Potential Factors in Amyloid Plaque Formation. *J. Neurosci.* **2006**, *26*, 10129.
(71) López, A.; Aparicio, N.; Pazos, M. R.; Grande, M. T.; Barreda-Manso, M. A.; Benito-Cuesta, I.; Vázquez, C.; Amores, M.; Ruiz-Pérez, G.; García-García, E.; Beatka, M.; Tolón, R. M.; Dittel, B. N.; Hillard, C. J.; Romero, J. Cannabinoid CB2 Receptors in the Mouse Brain: Relevance for Alzheimer's Disease. *J. Neuroinflammation* **2018**, *15*, 158.
(72) Incubation of cells with **3b** (0.5 μM) did not show any obvious signs of cell suffering (i.e., membrane blebbing, cell detachment, pyknotic nuclei) for the duration of the entire treatment (up to 2 h).
(73) Imaging experiments were performed at 22 °C to minimize internalization. Antagonist **3a** would not induce internalization but was not considered for microscopy due to poor performance in FACS.
(74) Kansy, M.; Senner, F.; Gubernator, K. Physicochemical High Throughput Screening: Parallel Artificial Membrane Permeation Assay in the Description of Passive Absorption Processes. *J. Med. Chem.* **1998**, *41*, 1007.
(75) The abundance CB_2R on internal membranes is well established. Labeling of intracellular CB_2R necessitates the development of membrane-permeant fluorescent probes by attachment of uncharged dyes to ligand **1**: den Boon, F. S.; Chameau, P.; Schaafsma-Zhao, Q.; van Aken, W.; Bari, M.; Oddi, S.; Kruse, C. G.; Maccarrone, M.; Wadman, W. J.; Werkman, T. R. Excitability of Prefrontal Cortical Pyramidal Neurons Is Modulated by Activation of Intracellular Type-2 Cannabinoid Receptors. *Proc. Natl. Acad. Sci. U. S. A.* **2012**, *109*, 3534.

https://dx.doi.org/10.1021/jacs.0c05587
J. Am. Chem. Soc. 2020, 142, 16953−16964